Electronic Supplementary Material (ESI) for Physical Chemistry Chemical Physics.

Electronic supplementary information (ESI): Density functional study of phase stabilities and Raman spectra of Yb_2O_3, Yb_2SiO_5 and $Yb_2Si_2O_7$ under pressure

Takafumi Ogawa,*[a] Noriko Otani,[a] Taishi Yokoi,[b] Craig A. J. Fisher,[a] Akihide Kuwabara,[a,c] Hiroki Moriwake,[a,c] Masato Yoshiya,[a,d] Satoshi Kitaoka,[b] and Masasuke Takata[a,b]

1 Dependence of Raman spectra on hydrostatic pressure

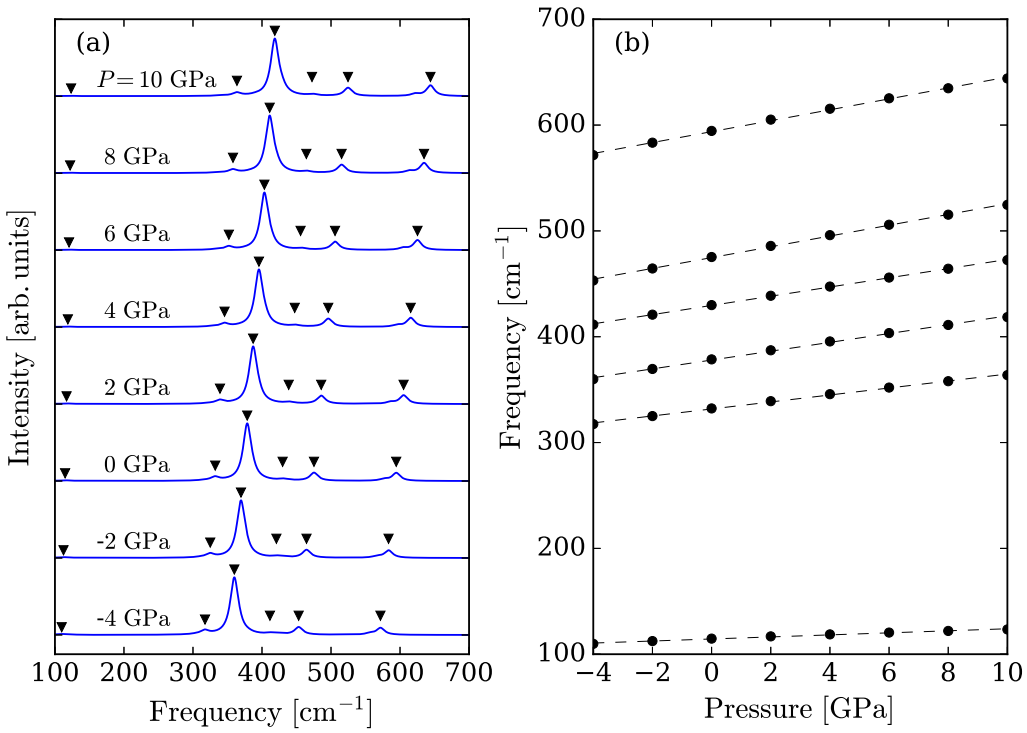

Fig. S1 Dependence of (a) Raman spectra and (b) peak positions of C-type Yb_2O_3 on hydrostatic pressure.

[a] *Nanostructures Research Laboratory, Japan Fine Ceramics Center, Nagoya 456-8587, Japan. E-mail: t_ogawa@jfcc.or.jp*
[b] *Materials Research and Development Laboratory, Japan Fine Ceramics Center, Nagoya 456-8587, Japan.*
[c] *Center for Materials Research by Information Integration, National Institute for Materials Science, Tsukuba 305-0047, Japan*
[d] *Department of Adaptive Machine Systems, Osaka University, Osaka 565-0871, Japan*

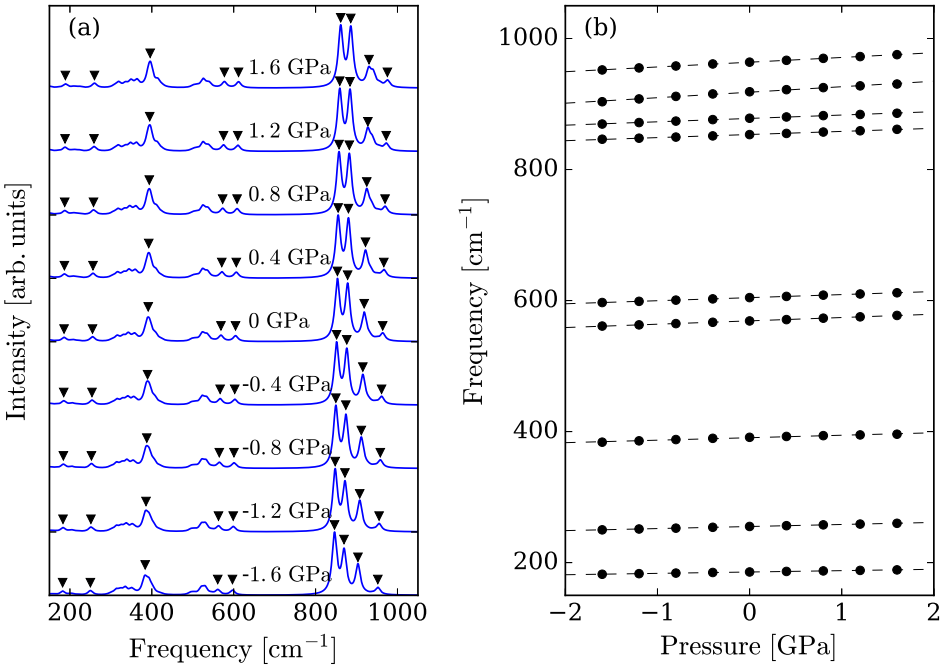

Fig. S2 Dependence of (a) Raman spectra and (b) peak positions of X_2-Yb_2SiO_5 on hydrostatic pressure.

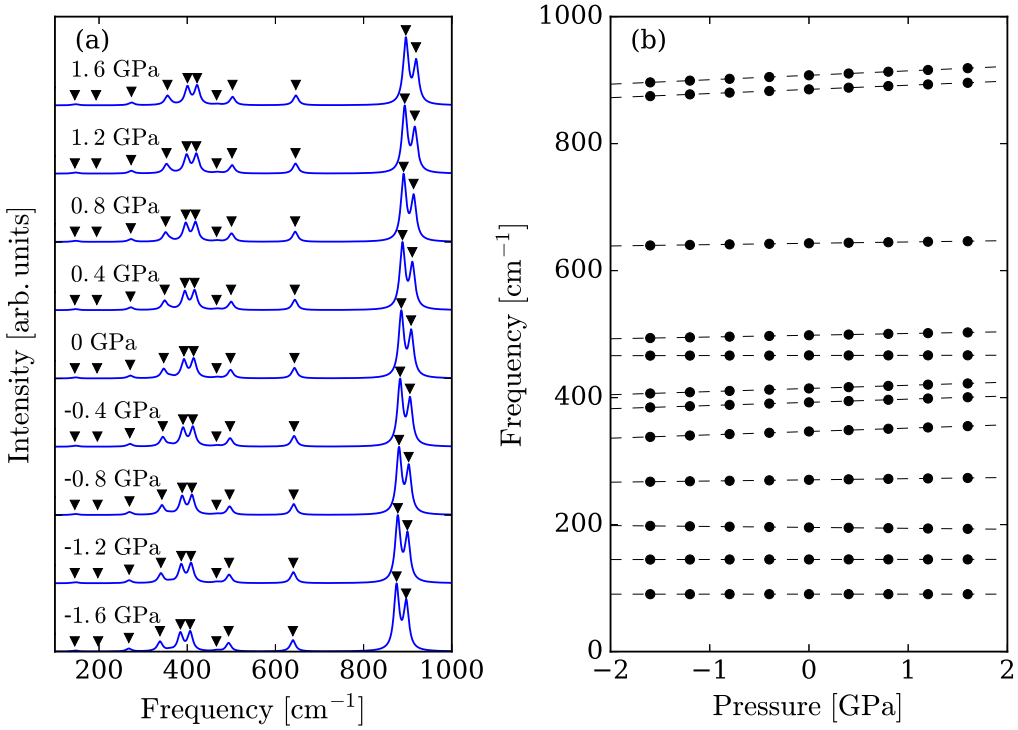

Fig. S3 Dependence of (a) Raman spectra and (b) peak positions of β-$Yb_2Si_2O_7$ on hydrostatic pressure.

2 Vibrations of Si_xO_y tetrahedral units in Yb_2SiO_5 and $Yb_2Si_2O_7$

The parameter used to measure maximum deviation in a bond length during vibration is defined in the manuscript as

$$\Delta l_{ij} = \frac{\boldsymbol{r}_{ij}{}^2 - \boldsymbol{r}_{ij}^{0\,2}}{r_{ij}^0 A}. \tag{1}$$

Since expressing the interatomic vector by the atomic positions and vibrational displacement vectors leads to

$$\boldsymbol{r}_{ij} = (\boldsymbol{r}_j^0 + \boldsymbol{u}_j) - (\boldsymbol{r}_i^0 + \boldsymbol{u}_i) = \boldsymbol{r}_{ij}^0 + \boldsymbol{u}_j - \boldsymbol{u}_i, \tag{2}$$

the parameter, Δl_{ij}, can be rewritten as

$$\Delta l_{ij} = 2\frac{\boldsymbol{r}_{ij}^0 \cdot (\boldsymbol{u}_j - \boldsymbol{u}_i)}{r_{ij}^0 A} + \frac{(\boldsymbol{u}_j - \boldsymbol{u}_i)^2}{r_{ij}^0 A}. \tag{3}$$

The second term on the right hand side of this equation vanishes when A is sufficiently smaller than r_{ij}^0 ($A/r_{ij}^0 \to 0$), leading to a converged value of Δl_{ij} in the limit of small A. To confirm this behaviour, the dependence of Δl_{ij} on A is examined for a mode of X_2-Yb_2SiO_5 as shown in Fig. S4. From the figure, we can see that the Δl_{ij} changes slightly for $A < 10^{-2}$. In this study, we used $A = 10^{-3}$ to calculate Δl_{ij}. The bond lengths between Si and O atoms and vibrational amplitudes, u_i^2/A^2 and Δl_{ij}, for characteristic modes with frequencies above 600 cm^{-1} are shown in Figs. S5 – S10, where the structural pictures of Si_xO_y were drawn using VESTA[1] and Raman spectra which were broadened by 7.0 and 0.05 cm^{-1} wide Lorentzians are shown by blue and red lines, respectively. The bond lengths in Si_3O_{10} and SiO_4 units in α-$Yb_2Si_2O_7$ are summarised in Table S1.

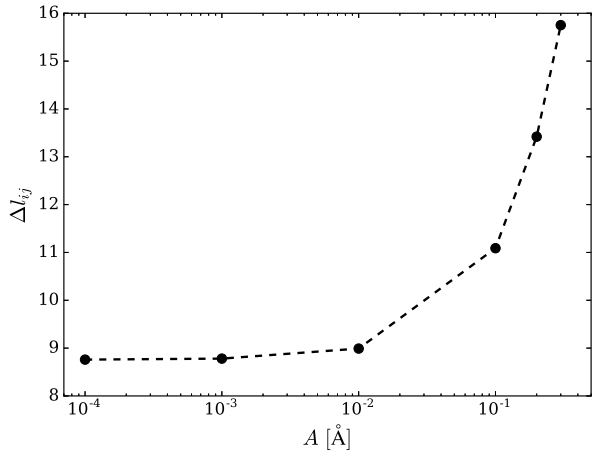

Fig. S4 Dependence of maximum deviations in a bond length, Δl_{ij}, on an amplitude, A, for the Si-O4 bond in X_2-Yb_2SiO_5 for the 853 cm^{-1} peak, shown in Fig. S5 (f).

References

1 K. Momma, F. Izumi, *J. Appl. Crystallogr.*, 2011, **44**, 1272–1276.

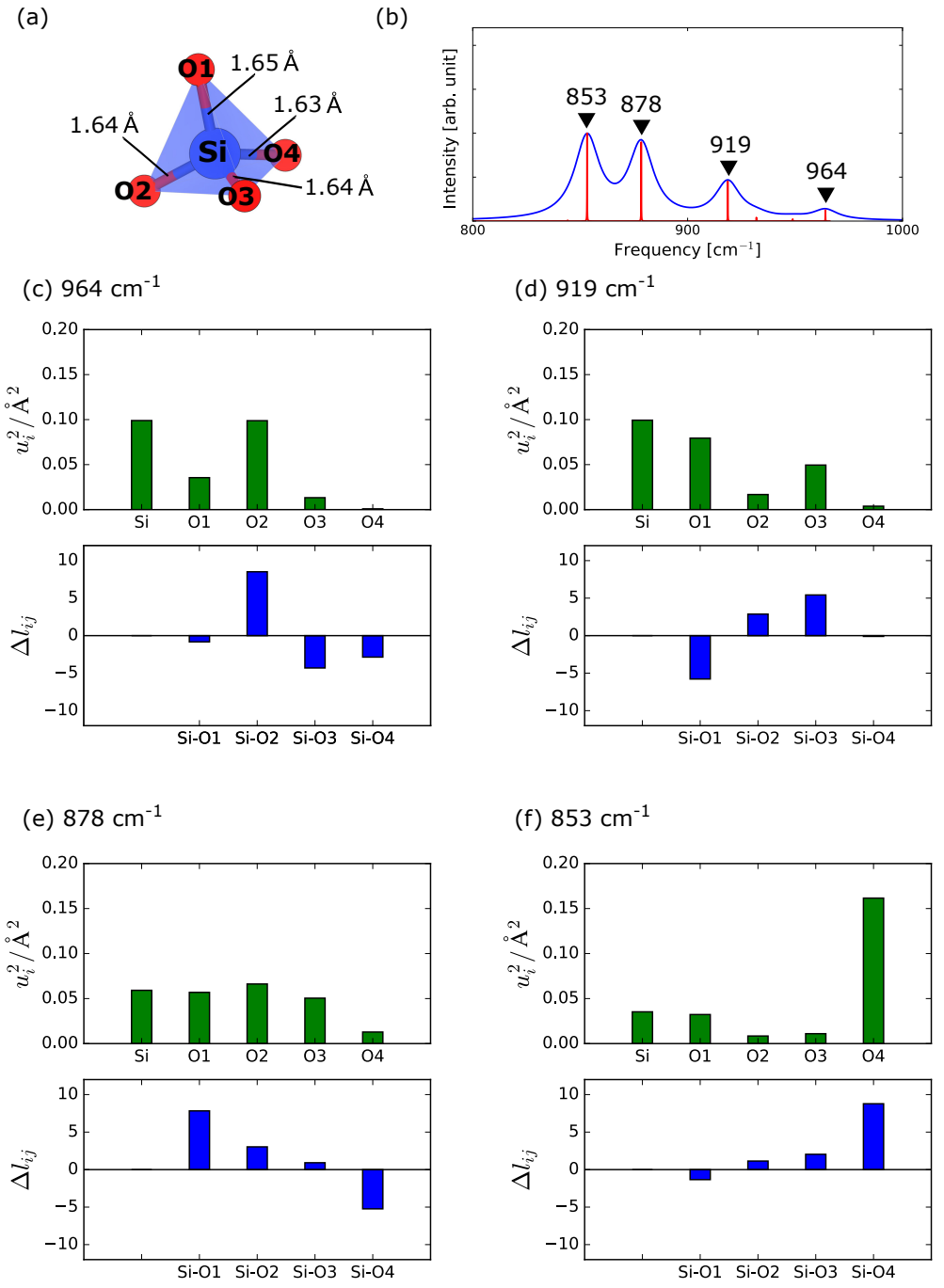

Fig. S5 (a) Structure of the SiO_4 unit in X_2-Yb_2SiO_5, (b) high frequency range of the calculated Raman spectrum of X_2-Yb_2SiO_5, and (c-f) vibrational amplitudes and Δl_{ij} for the normal modes at 964, 919, 878, and 853 cm^{-1}, respectively.

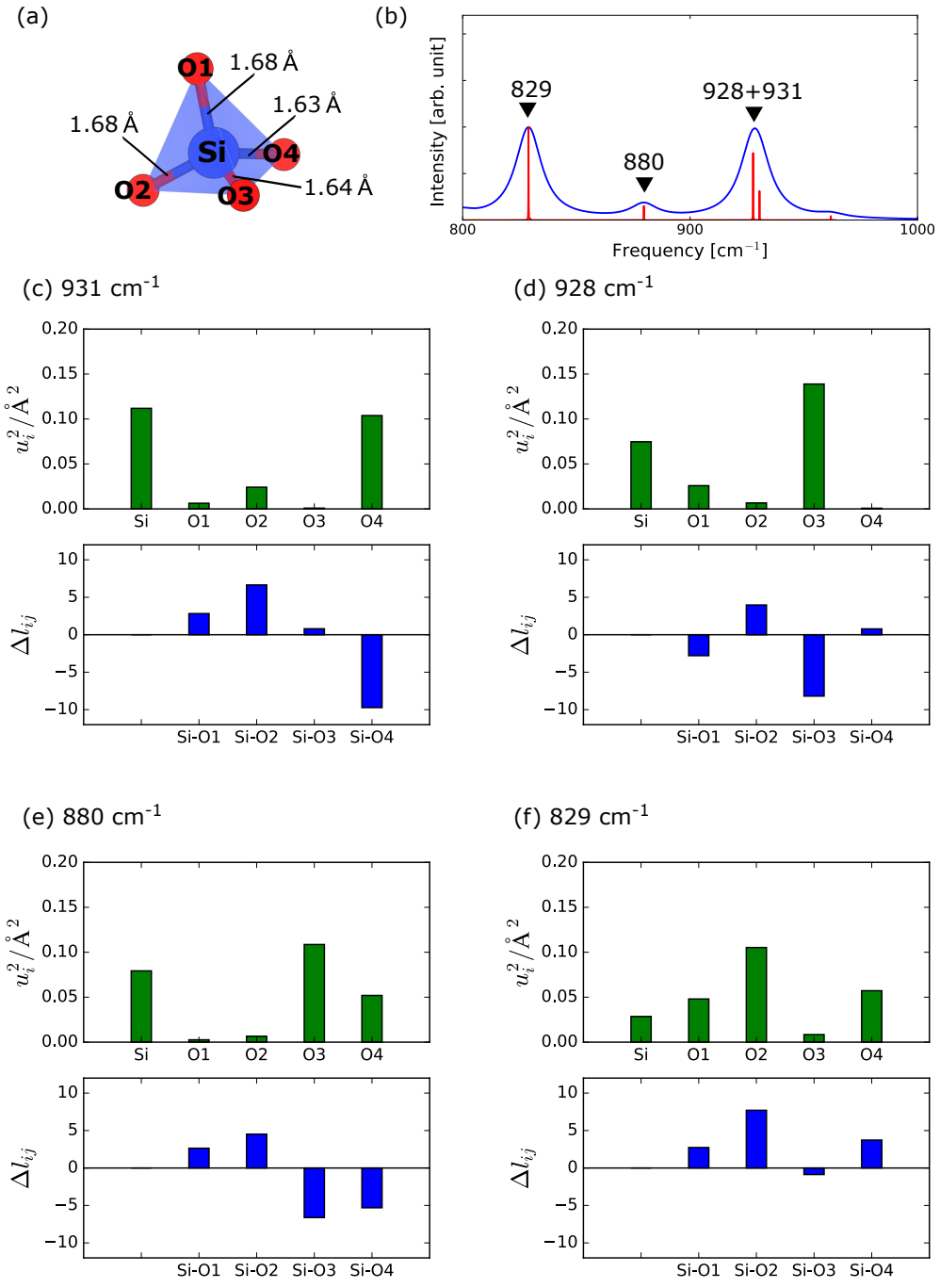

Fig. S6 (a) Structure of the SiO_4 unit in X_1-Yb_2SiO_5, (b) high frequency range of the calculated Raman spectrum of X_1-Yb_2SiO_5, and (c-f) vibrational amplitudes and Δl_{ij} for the normal modes at 931, 928, 880, and 829 cm^{-1}, respectively.

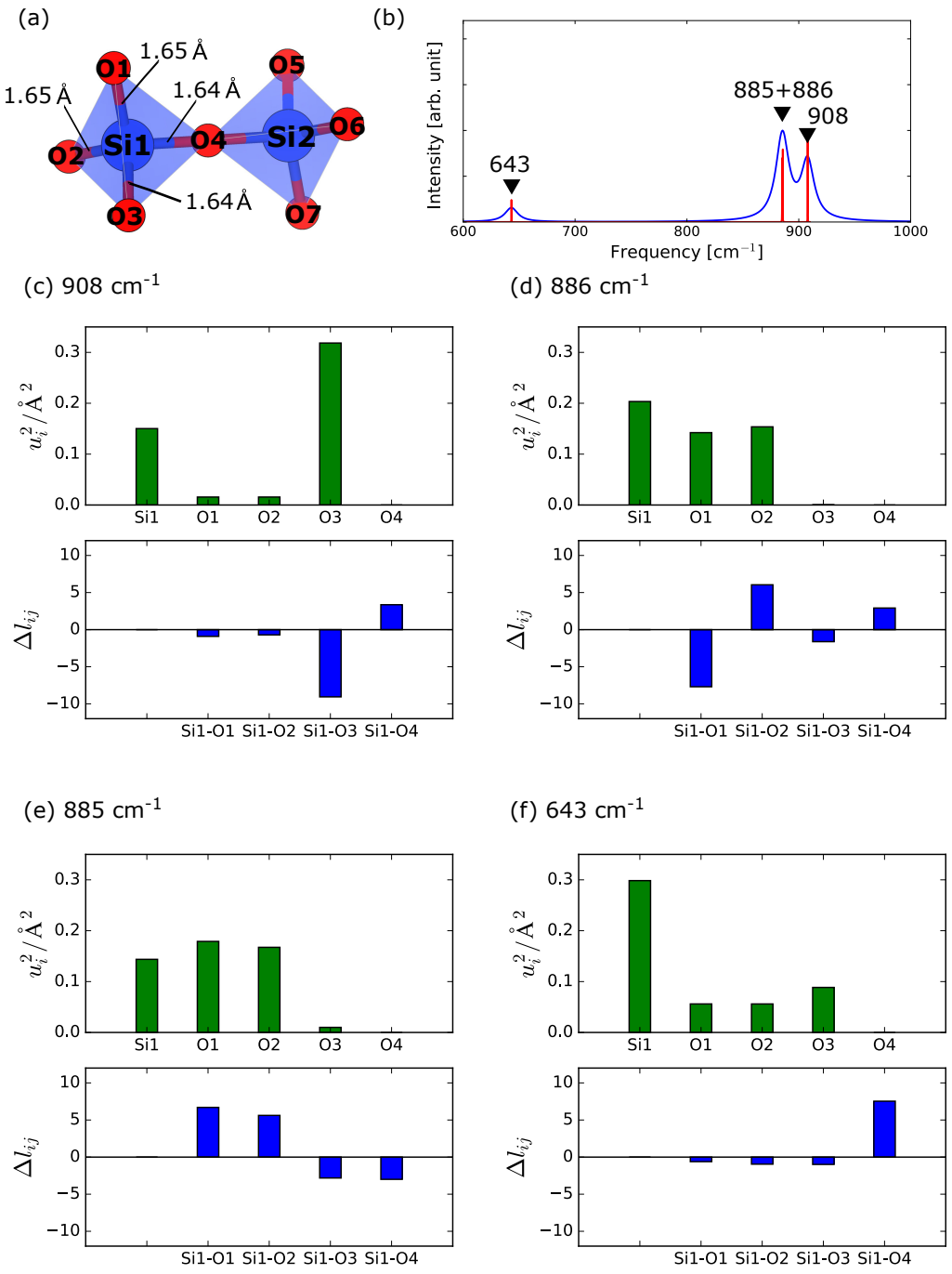

Fig. S7 (a) Structure of the Si_2O_7 unit in β-$Yb_2Si_2O_7$, (b) high frequency range of the calculated Raman spectrum of β-$Yb_2Si_2O_7$, and (c-f) vibrational amplitudes and Δl_{ij} for the normal modes at 908, 886, 885, and 643 cm^{-1}, respectively.

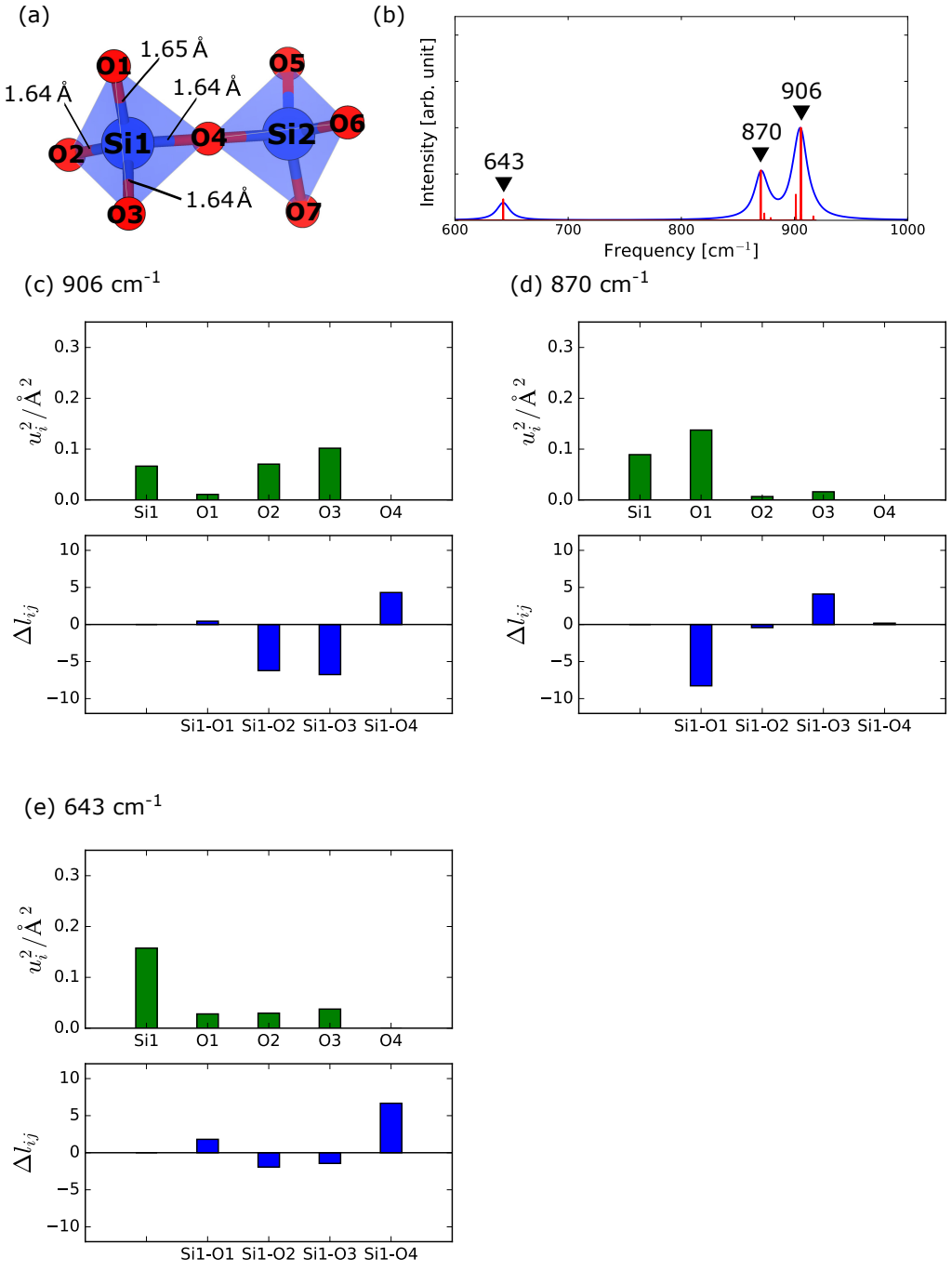

Fig. S8 (a) Structure of the Si_2O_7 unit in γ-$Yb_2Si_2O_7$, (b) high frequency range of the calculated Raman spectrum of γ-$Yb_2Si_2O_7$, and (c-e) vibrational amplitudes and Δl_{ij} for the normal modes at 906, 870, and 643 cm^{-1}, respectively.

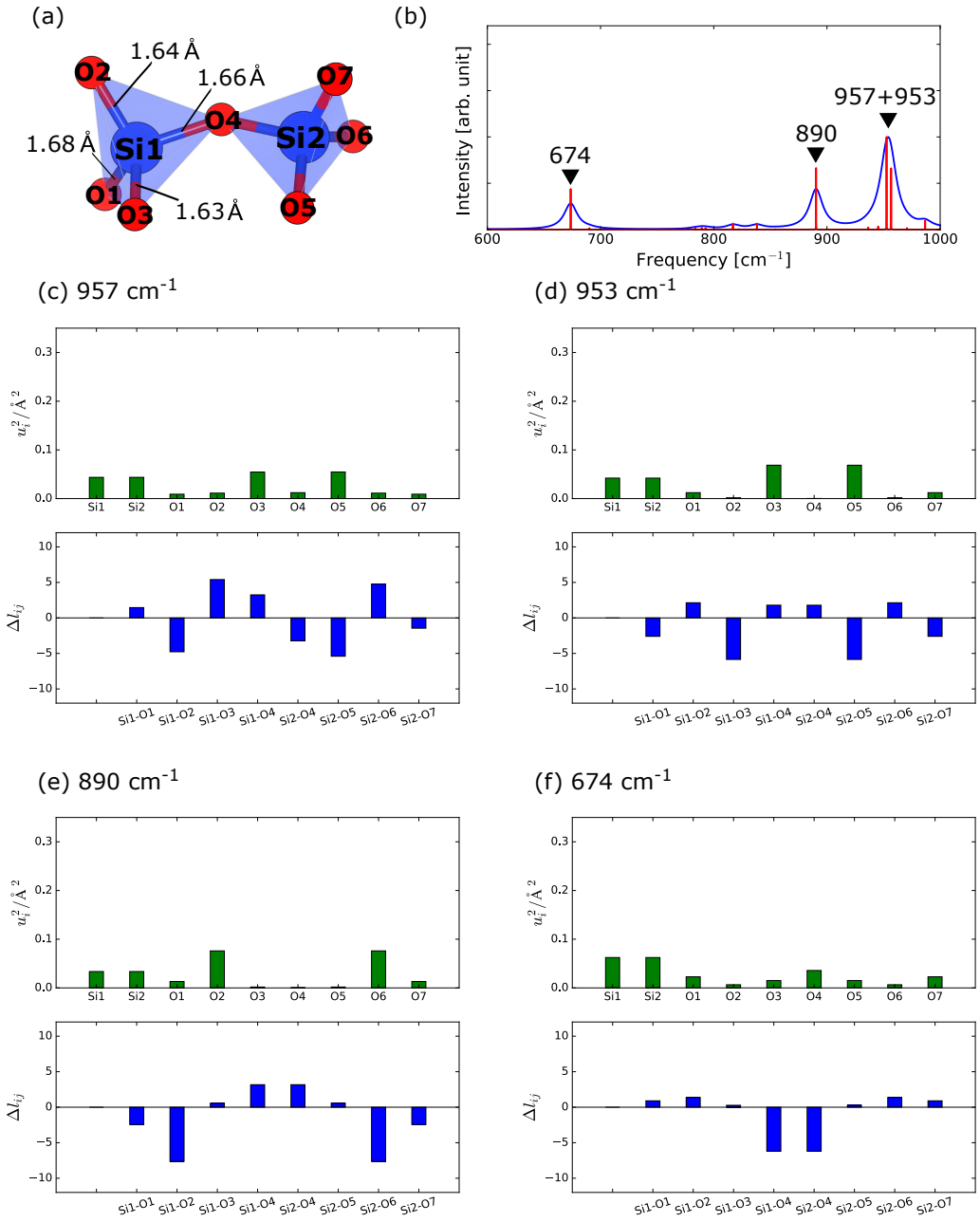

Fig. S9 (a) Structure of the Si_2O_7 unit in X-$Yb_2Si_2O_7$, (b) high frequency range of the calculated Raman spectrum of X-$Yb_2Si_2O_7$, and (c-f) vibrational amplitudes and Δl_{ij} for the normal modes at 957, 953, 890, and 674 cm^{-1}, respectively.

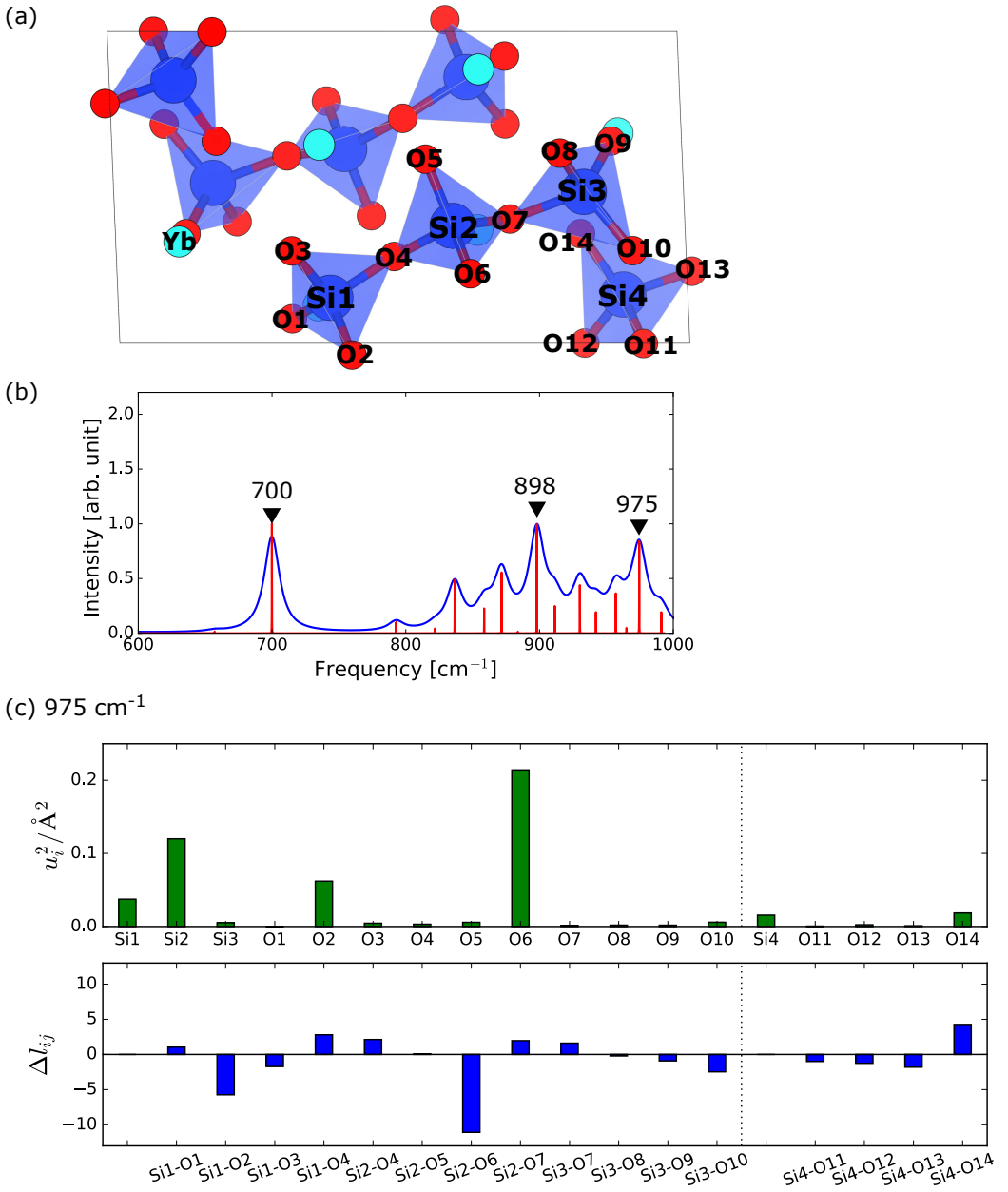

Fig. S10 (a) Structure of the Si_2O_7 unit in α-$Yb_2Si_2O_7$, (b) high frequency range of the calculated Raman spectrum of α-$Yb_2Si_2O_7$, and (c) vibrational amplitudes and Δl_{ij} for the normal mode at 975 cm^{-1}.

(e) 898 cm^{-1}

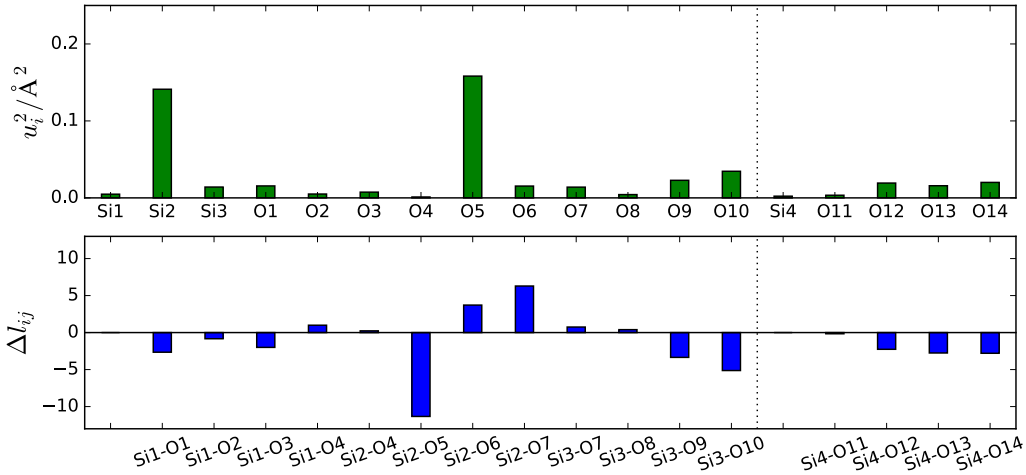

(f) 700 cm^{-1}

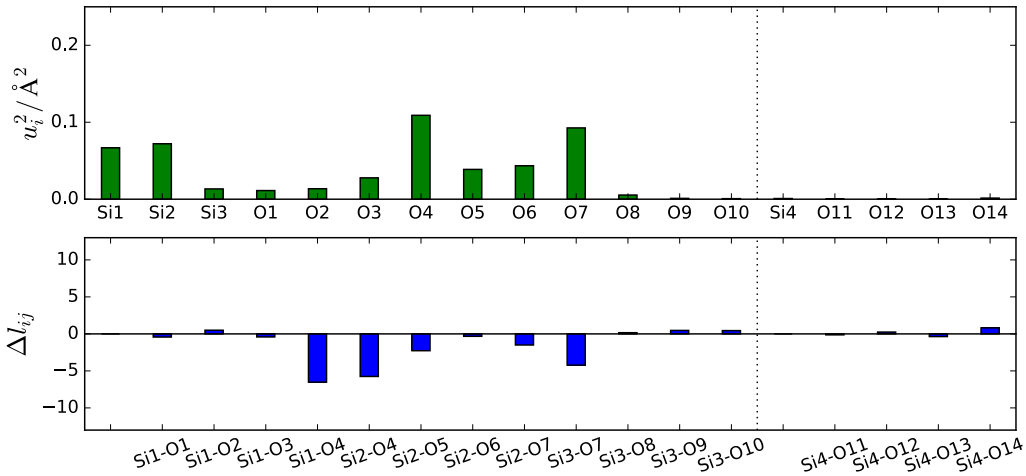

Fig. S10 (Continued) (d, e) normalized amplitudes and bond deviations for the normal modes at 898, and 700 cm^{-1}, respectively.

Table S1 Bond lengths between Si and O atoms in α-$Yb_2Si_2O_7$.

Bonds	Bond length [Å]
Si1-O1	1.62
Si1-O2	1.64
Si1-O3	1.66
Si1-O4	1.66
Si2-O4	1.66
Si2-O5	1.64
Si2-O6	1.62
Si2-O7	1.68
Si3-O7	1.75
Si3-O8	1.65
Si3-O9	1.63
Si3-O10	1.63
Si4-O11	1.67
Si4-O12	1.64
Si4-O13	1.62
Si4-O14	1.62